J. Cent. South Univ. (2019) 26: 2870−2877
DOI: https://doi.org/10.1007/s11771-019-4220-6

Springer

Calculation grid and turbulence model for numerical simulating pressure fluctuations in high-speed train tunnel

JI Peng(姬鹏)[1], WANG Tian-tian(王田天)[1, 2], WU Fan(伍钒)[1]

1. School of Traffic and Transportation Engineering, Central South University, Changsha 410075, China;
2. College of Mechanical and Vehicle Engineering, Hunan University, Changsha 410082, China

Abstract: Calculation grid and turbulence model for numerical simulating pressure fluctuations in a high-speed train tunnel are studied through the comparison analysis of numerical simulation and moving model test. Compared the waveforms and peak-peak values of pressure fluctuations between numerical simulation and moving model test, the structured grid and the SST k-ω turbulence model are selected for numerical simulating the process of high-speed train passing through the tunnel. The largest value of pressure wave amplitudes of numerical simulation and moving model test meet each other. And the locations of the largest value of the initial compression and expansion wave amplitude of numerical simulation are in agreement with that of moving model test. The calculated pressure at the measurement point fully conforms to the propagation law of compression and expansion waves in the tunnel.

Key words: high-speed train; calculation grid; turbulence model; tunnel; pressure fluctuations

Cite this article as: JI Peng, WANG Tian-tian, WU Fan. Calculation grid and turbulence model for numerical simulating pressure fluctuations in a high-speed train tunnel [J]. Journal of Central South University, 2019, 26(10): 2870−2877. DOI: https://doi.org/10.1007/s11771-019-4220-6.

1 Introduction

Pressure fluctuations in a high-speed train tunnel are a focus of attention [1]. The pressure fluctuations are sensitive to calculation grid and turbulence model in numerical simulation [2, 3]. Calculation grid and turbulence model are selected by comparing the data between numerical simulation and moving model test in this manuscript.

Unlike wind tunnel test, moving model test can accurately simulate the relative motion between the high-speed train, the ground and the tunnel [4]. KIM et al [5] and SOPER [6] experimentally studied the flow field and the air slipstream development around train. BELLENOUE et al [7] and RICCOA et al [8] studied the characteristics of pressure waves in a high-speed train tunnel based on moving model tests. ZHANG et al [9] and ENDO et al [10] studied oblique tunnel portal effect on pressure fluctuations of a high-speed train passing through a tunnel by using moving model test.

Numerical simulation is an important research approach in the process of design and analysis. With the rapid improvement of computing power and the continuous development of numerical calculation methods, research on the aerodynamics of high-speed trains/tunnels have expanded from one-dimensional to three-dimensional numerical simulations [11]. Due to the large calculation in the high-speed tunnel/train coupled aerodynamic simulation, the more practical model is to use

Received date: 2018-06-05; **Accepted date:** 2018-07-19
Corresponding author: WANG Tian-tian, PhD; E-mail: wangtiantian@csu.edu.cn; ORCID: 0000-0003-0137-7881

Reynolds average Navier-Stokes (RANS) in combination with different types of turbulence closure models. At the same time, the relative motion between train and tunnel is achieved through the sliding grid method and the numerical calculation of the tunnel/train coupled pressure is carried out [11, 12]. WANG et al [13, 14] and ZHANG et al [15] studied the reduction issues of the train/tunnel pressure fluctuations based on RANS method. Recently, detached eddy simulation (DES) and large eddy simulation (LES) have been used to simulate the airflow around high-speed trains [16−19]. However, due to its computational complexity, there are still some difficulties in numerical simulation of the aerodynamic performance in high-speed train tunnels. In this manuscript, the RANS and the sliding grid method are adopted for numerical simulating the pressure fluctuations in a high-speed train tunnel.

2 Program setup

Through comparison analysis of numerical simulation and moving model test, the calculation grid and turbulence model which effectively simulate the pressure fluctuations in a high-speed train tunnel can be obtained. The plans of numerical simulation and moving model test are set below.

2.1 Moving model test

The moving model test is carried out on the 'Aerodynamic Characteristics Moving Model Test System' of Central South University, which is the largest moving model test system for simulating high-speed train movement in the world at present. The test system has obtained the qualification of China Metrology Accreditation (CMA) and the certificate number is 2014002479 K. Ejection launch approach is selected and the model train is sliding without power after ejection. For the measurement of pressure fluctuations, Honeywell DC030NDC4 pressure sensors are chosen in this test. The detailed introduction for the test platform can be found in Ref. [4, 9].

A certain type of high-speed train in China with three cars is adopted in the test. The total length of the high-speed train is 79.77 m. The real picture of the train model is shown in Figure 1. The 70 m^2 standard tunnel is adopted and the length is 350 m. The dimensional figure of the tunnel cross-section is shown in Figure 2. Three speeds are selected for the test: 250, 300 and 350 km/h. The tunnel surface measurement points are set at 79, 99 and 179 m to the tunnel entrance, respectively. The measurement points are all 3 m away from the ground. The pressures taken from the tunnel surface measurement points are relative pressure.

Figure 1 Model of high-speed train

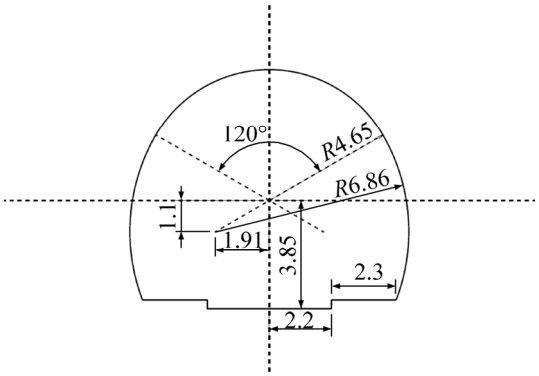

Figure 2 Tunnel cross-section dimension (Unit: m)

2.2 Numerical simulation

In this work, the RANS and the sliding grid method are adopted for numerical simulation by using Fluent commercial software. The train movement distance should keep the same in each calculation step. As a result, 0.012 s, 0.01 s and 0.00857 s are set as time-steps for 250, 300 and 350 km/h velocities, respectively. The standard format is selected for the pressure terms in the governing equations.

Two different types of calculation grids and five turbulence models are selected for numerical simulation study. Both the structured grid built by software Pointwise and the unstructured grid built by software Gambit are numerical verified by the experimental results. For the structured grid, the grid of bogies area is unstructured because the

bogies are very complex. Then the structured grid is adopted to other regions, including the area around train body, and the boundary layers of the train body surface and tunnel surface are set. The thickness of the first boundary layer grid is 1 mm and the total number of grid is 50 million.

Figure 3 shows the train head surface mesh of the structured grid. For the unstructured grid, the thickness of the first boundary layer grid is 1 mm and the total number of grid is 41 million. Figure 4 shows the train head surface mesh of the unstructured grid.

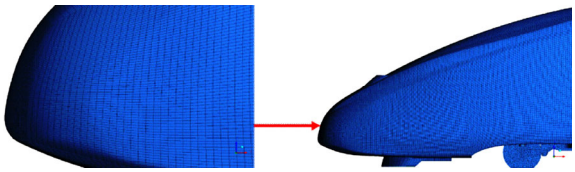

Figure 3 Surface mesh of structured grid

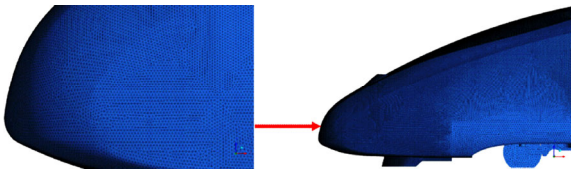

Figure 4 Surface mesh of unstructured grid

The real state around high-speed trains is a turbulent flow. At present, for the problem of engineering turbulence in train aerodynamics, the most widely used is the k-ω and k-ε two-equation turbulence in train aerodynamics, the most widely used is the k-ω and k-ε two-equation turbulence model series. In this manuscript, realizable k-ε, RNG k-ε, standard k-ε, SST k-ω, standard k-ω turbulence models in Fluent commercial software are selected for comparing the numerical simulation results of pressure fluctuations in a high-speed train tunnel.

The sliding mesh method is selected in this study and the moving speed is set as the train speed. The surface of the train, tunnel and ground are set as no-sliding wall boundary condition. The other boundary surfaces are set as pressure outlets. The schematic diagram of the boundary conditions can be found in Ref. [14].

3 Calculation grid and turbulence model selection

The waveforms and peak-peak values of pressure fluctuations measured and calculated from tunnel surface measurement points are selected for the comparison between numerical simulation results and moving model test data. Waveform is defined as the change curve of pressure with time. The first positive pressure wave and the first negative wave are defined as the initial compression wave and the initial expansion wave, respectively. The difference between the initial compression wave peak and the initial expansion wave peak is defined as peak-peak value. The process of high-speed train passing through the tunnel is simulated by the sliding mesh method.

3.1 Waveform

The 250, 300 and 350 km/h numerical simulation and measurement results of pressure fluctuations of 79 m measurement point of the tunnel surface are shown in Figures 5−7, respectively. The ke-rea, ke-rng, ke-stan, kw-sst and kw-stan in the figure represent realizable k-ε, RNG k-ε, standard k-ε, SST k-ω, standard k-ω turbulence models, respectively. The moment is set as the time origin when the high-speed train nose enters the tunnel. And the moment is set as the last moment

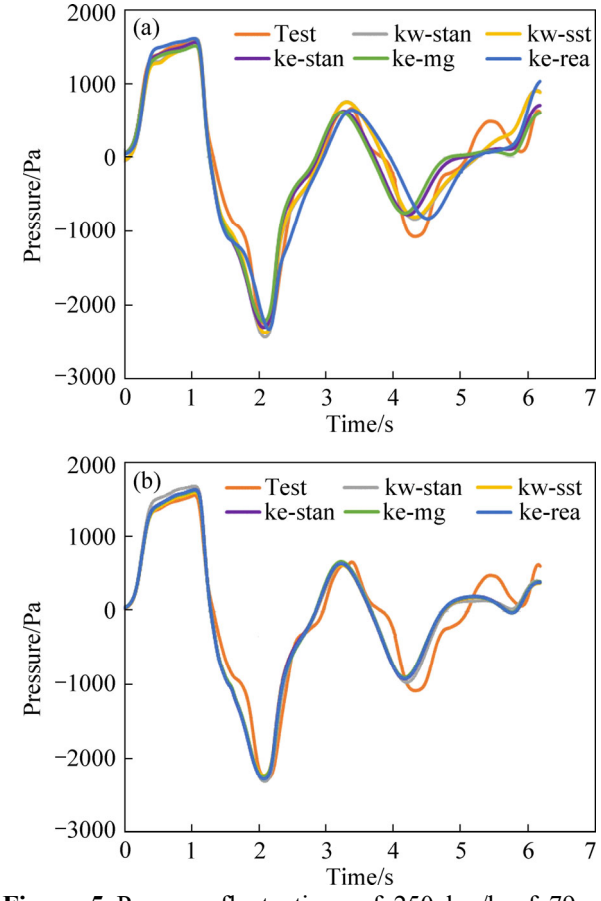

Figure 5 Pressure fluctuations of 250 km/h of 79 m: (a) Structured grid; (b) Unstructured grid

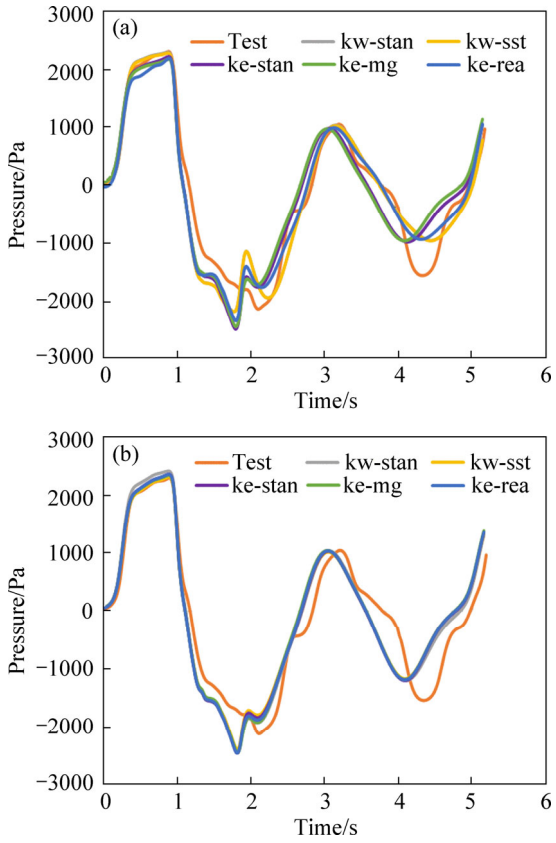

Figure 6 Pressure fluctuations of 300 km/h of 79 m: (a) Structured grid; (b) Unstructured grid

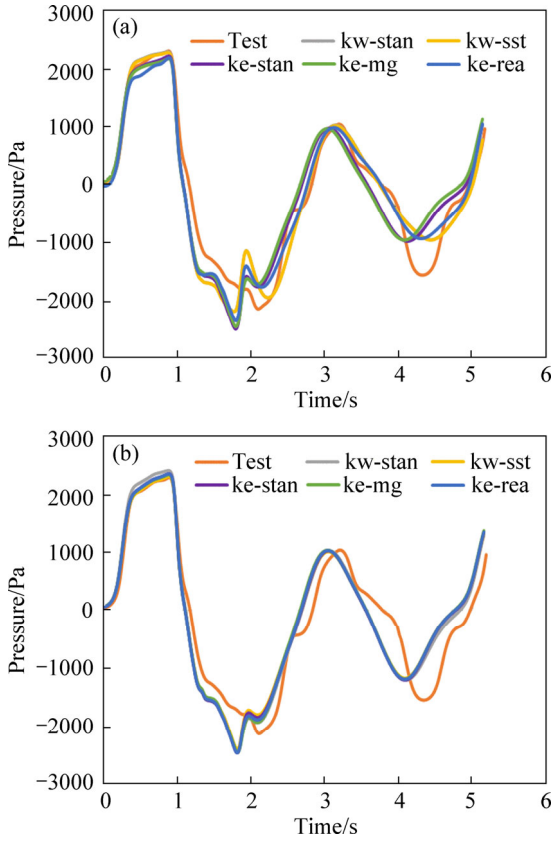

Figure 7 Pressure fluctuations of 350 km/h of 79 m: (a) Structured grid; (b) Unstructured grid

when the high-speed train tail exits the tunnel. The process time of the high-speed train passing through the tunnel at 250, 300 and 350 km/h are 6.18 s, 5.16 s and 4.42 s, respectively.

In the three figures, the pressure fluctuations of test and calculation are basically consistent. The initial compression wave waveform of the calculation is approximately identical to that of the test. The pressure fluctuations of different turbulence models are different from each other for the structured grid, while that for the unstructured grid are similar. The pressure waveforms of the experiment data have a certain delay compared to the numerical simulation results. The causes are explained carefully in Ref. [13]. As the waveforms of the test and calculation are basically consistent, the pressure peak-peak value is adopted to the further study.

3.2 Peak-peak value

Tables 1 and 2 show the pressure peak-peak value numerical errors of three tunnel surface measurement points at different operating speeds from the structured and unstructured grid, respectively. The pressure peak-peak value of the simulation results is defined as Psi and that of the experimental data is defined as Pex. The numerical error is defined as (Psi−Pex)/Pex.

Table 1 Pressure peak-peak value numerical errors of structured grid

Speed/ (km·h^{-1})	Model	Error		
		79 m	99 m	179 m
250	ke-rea	−2.3%	−7.4%	−20.4%
	ke-rng	2.7%	3.9%	8.9%
	ke-stan	−0.4%	0.7%	5.1%
	kw-sst	−3.1%	−2.9%	−1.9%
	kw-stan	−7.4%	−7.0%	−7.8%
300	ke-rea	2.7%	−0.8%	4.3%
	ke-rng	0.8%	1.7%	10.8%
	ke-stan	−1.2%	−0.9%	8.2%
	kw-sst	4.2%	−0.2%	1.6%
	kw-stan	1.7%	−2.8%	−1.6%
350	ke-rea	6.6%	−1.3%	1.1%
	ke-rng	6.6%	−2.9%	3.7%
	ke-stan	4.0%	−5.0%	1.3%
	kw-sst	0.3%	1.8%	−1.7%
	kw-stan	−3.7%	0.3%	−4.7%

Table 2 Pressure peak-peak value numerical errors of unstructured grid

Speed/ (km·h^{-1})	Model	Error		
		79 m	99 m	179 m
250	ke-rea	−2.2%	−2.7%	−1.6%
	ke-rng	−1.1%	−1.9%	−1.7%
	ke-stan	−2.3%	−3.0%	−1.3%
	kw-sst	−0.3%	−0.9%	0.7%
	kw-stan	−4.5%	−5.0%	−4.9%
300	ke-rea	−4.2%	−3.9%	5.2%
	ke-rng	−3.7%	−3.1%	5.4%
	ke-stan	−4.4%	−4.0%	4.9%
	kw-sst	−2.3%	−1.9%	6.8%
	kw-stan	−4.9%	−4.6%	3.7%
350	ke-rea	1.3%	−8.1%	−2.0%
	ke-rng	2.4%	−7.1%	−1.6%
	ke-stan	1.6%	−7.9%	−2.1%
	kw-sst	3.6%	−5.7%	−0.1%
	kw-stan	−0.3%	−7.4%	−3.0%

As can be seen from the two tables, the pressure peak-peak value of the SST *k*-*ω* turbulence model is the closest to that of the test among all turbulence models. The pressure peak-peak value numerical error of the structured grid adopted the SST *k*-*ω* turbulence model is less than 4.2% and that of the unstructured grid is more than 6.8%. The pressure peak-peak value numerical errors of other turbulence models are larger than 5.1%. For engineering applications, it is generally considered that the error between numerical simulation and experiment is less than 5%, which can be effectively simulated. As a result, the structured grid adopted the SST *k*-*ω* turbulence model is selected for numerical simulating pressure fluctuations in a high-speed train tunnel.

4 Program validation

The numerical simulation by using selected calculation grid and turbulence model are validated in two aspects: the locations of the largest value of pressure amplitude and measurement point pressure change Mach diagram.

4.1 Locations of largest value of pressure amplitude

Table 3 shows the numerical simulation results of the largest value of the initial compression wave amplitude defined as P_{c0} , the largest value of the initial expansion wave amplitude defined as P_{e0} and the corresponding locations along the direction of tunnel length defined as L_{c0} and L_{e0}. P_{c0} and P_{e0} represent the maximum pressure of the initial compression wave and the minimum pressure of the initial expansion wave without considering the reflection pressure waves at the tunnel exit, respectively. P_{c0}, P_{e0} and the corresponding locations along the direction of tunnel length vary with the speed of high speed train. In this study, 351 measurement points are distributed along the direction of tunnel length (1 m apart). The maximum pressure of all measurement points is identified as P_{c0}. The location of that measurement point is identified as L_{c0}. P_{e0} and L_{e0} are obtained in the same way.

Table 3 Largest value of pressure wave amplitudes and corresponding locations of numerical simulation

Speed/(km·h^{-1})	P_{c0}/Pa	P_{e0}/Pa	L_{c0}/m	L_{e0}/m
250	1571.9	−2367.5	83	111
300	2245.5	−3589.6	87	136
350	3065.4	−5057.6	91	143

As can be seen from the Table 3, L_{c0} and L_{e0} are 83−91 m away from the tunnel entrance and 110−143 m away from the tunnel entrance, respectively. And L_{c0} and L_{e0} expand into the tunnel with the increase of the speed.

Table 4 shows the moving model test results of the maximum and minimum pressures of three measurement points of the tunnel surface. The maximum pressure is the peak value of the initial compression wave at the location of the measurement point and the minimum pressure is

Table 4 Largest value of pressure amplitudes of tunnel surface measurement points of moving model test

Speed/ (km·h^{-1})	Symbol	Pressure/Pa		
		79 m	99 m	179 m
250	P_c	1587.487	1570.314	1524.198
	P_e	−2258.48	−2335.97	−1234.75
300	P_c	2303.449	2313.961	2266.441
	P_e	−2338.35	−3349.58	−3210.7
350	P_c	3102.611	3166.165	3134.851
	P_e	−2784.04	−3096.07	−4898.22

that of the initial expansion wave. The P_c and P_e represent the maximum and minimum pressure in the table, respectively.

For 250 km/h, as the pressure maximum of 79 m is larger than that of 99 m, the location of the largest value of the initial compression wave amplitude should be near the 79 m measurement point. For 300 km/h, as the pressure maximum of 99 m is close to that of 79 m, the largest value of the initial compression wave amplitude location should be in the middle of the two measurement points. For 350 km/h, the pressure maximum of 99 m is larger than that of 79 m and 179 m, the location should be near the 99 m measurement point. These conclusions are in agreement with the conclusions of Table 3. The location of the largest value of the initial expansion wave amplitude can be analyzed in the same way. As a result, the numerical simulation results are reliable. That is to say, the selected calculation grid and turbulence model can effectively simulate pressure fluctuations as the high-speed train passes the tunnel.

4.2 Pressure change Mach diagram

The air flow around the train is confined by the surface of the tunnel wall and train to form compression waves and expansion waves when a high-speed train head and tail enters and exits the tunnel. The two waves propagate at sound speed in the tunnel, resulting the pressure fluctuations inside the tunnel. Analyzing the relationship between the pressure fluctuations and the compression wave and expansion wave in the tunnel can also indirectly validate the accuracy of the numerical simulation.

Figure 8 is a numerical simulation pressure change Mach diagram of 79 m measurement point of 250 km/h. This figure can clearly analyze the relationship between the tunnel pressure change process and wave propagation. The upper figure is a Mach diagram and the red and blue curves represent compression and expansion wave, respectively. The lower figure shows pressure change with time. For a better description, the turning point of the pressure change caused by the air wave propagation process is marked with the serial number A-H. The time at which the train head enters the tunnel is defined as the start of time and the time that the train tail exits the tunnel is the end of time.

When the train head enters the tunnel, under the extrusion of the train and the tunnel wall,

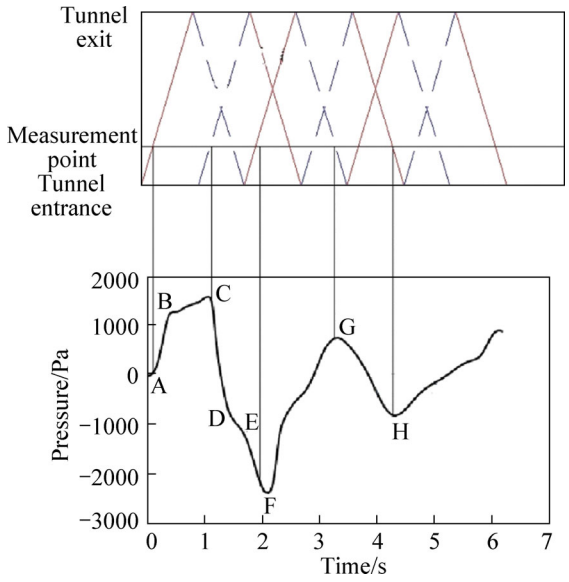

Figure 8 Pressure change Mach diagram of 250 km/h of 79 m

pressure rises rapidly to produce a compression wave and propagate forward at sound speed. When it reaches the position A in the figure, the initial compression wave is transmitted to the 79 m measurement point and pressure at this measurement point begins to increase. The entire A-C process is the propagation period of the initial compression wave. This period can be divided into two parts: pressure rises rapidly (AB segment) and rises slowly (BC segment). The reason for the first part is the streamline part of the train head enters the tunnel, the blocking ratio will continuously increase during the process, so pressure at the measurement point increases rapidly. After the streamline part of the train head completely enters the tunnel, the blocking ratio will not change during the process of the train body part entering the tunnel. However, the surrounding air temperature will increase slightly because of the friction effects, which leads to sound speed increase slightly. The newly generated compression wave will catch up with the compression wave propagating in the front, and pressure at the measurement point will increase slowly. When reaching the position C, due to the train tail entering the tunnel, the expansion wave formed by the negative pressure of the train tail also propagates forward at sound speed and reaches the measurement point. As a result, pressure at the measurement point begins to drop sharply and gradually becomes a negative pressure (CD segment). When the train reaches the measurement

point (corresponding to point E), pressure continues to decrease sharply until the train tail reaches the measurement point (corresponding to point F). At this time, negative pressure value reaches its maximum. When the compression wave propagates to the tunnel exit, on the one hand, micro-pressure waves are formed and on the other hand, it will be converted into an expansion wave. As the train tail expansion wave arrives at the tunnel exit and is converted back into a compression wave, pressure at the measurement point reaches the position G. Afterwards, pressure drops again and picks up again.

Although only one measurement point of tunnel surface is selected, it can represent the pressure variation law of other parts of the tunnel, and only the magnitude and time of the impact are different. The above analysis shows that the calculated pressure waveforms fully conforms to the propagation law of the expansion wave and compression wave, which shows the accuracy of the numerical simulation results.

5 Conclusions

By comparing the waveforms and peak-peak values of pressure fluctuations between numerical simulation results and moving model test data, the structured grid and the SST k-ω turbulence model are selected for numerical simulating the pressure fluctuations in a high-speed train tunnel.

1) The largest value of pressure wave amplitudes of numerical simulation results and moving model test data meet each other, with differences less than 4.2%.

2) The locations of the largest value of the initial compression and expansion wave amplitude of numerical simulation are in agreement with that of moving model test inference.

3) The propagation law of the expansion wave and compression wave in the tunnel are obtained. The calculated pressure waveform fully conforms to the propagation law, which shows the accuracy of the numerical simulation results.

References

[1] TIAN Hong-qi. Train aerodynamics [M]. Beijing: China Railway Publish House, 2007. (in Chinese)

[2] WANG Tian-tian, JIANG Chong-wen, GAO Zhen-xun, LEE Chun-hian. Numerical simulation of sand load applied on high-speed train in sand environment [J]. Journal of Central South University, 2017, 24: 442−447. DOI: 10.1007/s11771-017-3446-4.

[3] TAO Yu, YANG Ming-zhi, QIAN Bo-sen, WU Fan, WANG Tian-tian. Numerical and experimental study on ventilation panel models in a subway passenger compartment [J]. Engineering, 2019, 5: 329−336. DOI: 10.1016/j.eng.2018.12.007.

[4] ZHOU Dan, TIAN Hong-qi, ZHANG Jian, YANG Ming-zhi. Pressure fluctuations induced by a high-speed train passing through a station [J]. Journal of Wind Engineering and Industrial Aerodynamics, 2014, 135: 1−9. DOI: 10.1016/j.jweia.2014.09.006.

[5] KIM J Y, KIM K Y. Experimental and numerical analyses of train-induced unsteady tunnel flow in subway [J]. Tunnelling and Underground Space Technology, 2007, 22: 166−172. DOI: 10.1016/j.tust.2006.06.001.

[6] SOPER D, BAKER C J, STERLING M. Experimental investigation of the slipstream development around a container freight train using a moving model facility [J]. Journal of Wind Engineering and Industrial Aerodynamics, 2014, 135: 105−117. DOI: 10.1016/j.jweia.2014.10.001.

[7] BELLENOUE M, MORINIERE V, KAGEYAMA T. Experimental 3-D simulation of the compression wave, due to train–tunnel entry [J]. Journal of Fluids and Structures, 2002, 16: 581−595. DOI: 10.1006/jfls.2002.044.

[8] RICCOA P, BARONB A, MOLTENI P. Nature of pressure waves induced by a high-speed train travelling through a tunnel [J]. Journal of Wind Engineering and Industrial Aerodynamics, 2007, 95: 781−808. DOI: 10.1016/j.jweia.2007.01.008.

[9] ZHANG Lei, YANG Ming-zhi, LIANG Xi-feng, ZHANG Jian. Oblique tunnel portal effects on train and tunnel aerodynamics based on moving model tests [J]. Journal of Wind Engineering and Industrial Aerodynamics, 2017, 167: 128−139. DOI: 10.1016/j.jweia.2017.04.018.

[10] ENDO H, MEGURO F, OTA M. Small model experiment on the gradient of pressure wave by entering the tunnel of a conventional limited express [J]. Proceedings of the Japan Society for Photoelasticity, 2014, 14: 42−47. DOI: 10.11395/jjsem.14.s42.

[11] ZHOU Dan. Research on the long tunnel and tunnel group's aerodynamic algorithm and its application [D]. Changsha: Central South University, 2007. (in Chinese)

[12] OGAWA T, FUJII K. Numerical investigation of three-dimensional compressible flows induced by a train moving into a tunnel [J]. Computers and Fluids, 1997, 26: 565−585. DOI: 10.1016/S0045-7930(97)00008-X.

[13] WANG Tian-tian, LEE Chun-xian, YANG Ming-zhi. Influence of enlarged section parameters on pressure fluctuations in a high-speed train tunnel [J]. Journal of Central South University, 2018, 25: 2831−2840. DOI: 10.1007/s11771-018-3956-8.

[14] WANG Tian-tian, WU Fan, YANG Ming-zhi, JI Peng, QIAN Bo-sen. Reduction of pressure fluctuations in a high-speed train tunnel by cross-section increase [J]. Journal of Wind Engineering and Industrial Aerodynamics, 2018, 183: 235−242. DOI: 10.1016/j.jweia.2018.11.001.

[15] ZHANG Lei, HUROW K, STOLL N, LIU Hui. Influence of

the geometry of equal-transect oblique tunnel portal on compression wave and micro-pressure wave generated by high-speed trains entering tunnels [J]. Journal of Wind Engineering and Industrial Aerodynamics, 2018, 178: 1−17. DOI: 10.1016/j.jweia.2018.05.003.

[16] HEMIDA H, GIL N, BAKER C J. LES of the slipstream of a rotating train [J]. Journal of Fluids Engineering, 2010, 132: 1031−1039. DOI: 10.1115/1.4001447.

[17] CHEN Jing-wen, GAO Guang-jun, ZHU Chun-li. Detached-eddy simulation of flow around high-speed train on a bridge under cross winds [J]. Journal of Central South University, 2016, 23: 2735−2746. DOI: 10.1007/s11771-016-3335-2.

[18] MALEKI S, BURTON D, THOMPSON M C. Assessment of various turbulence models (ELES, SAS, URANS and RANS) for predicting the aerodynamics of freight train container wagons [J]. Journal of Wind Engineering and Industrial Aerodynamics, 2017, 170: 68−80. DOI: 10.1016/j.jweia.2017.07.008.

[19] MORDEN J A, HEMIDA H, BAKER C J. Comparison of RANS and detached eddy simulation results to wind-tunnel data for the surface pressures upon a class 43 high-speed train [J]. Journal of Fluids Engineering, 2015, 137: 1−9. DOI: 10.1115/1.40292.

(Edited by HE Yun-bin)

中文导读

高速列车过隧道压力波动数值模拟中的计算网格及湍流模型研究

摘要：通过动模试验和数值模拟的对比分析，研究了不同计算网格和湍流模型模拟高速列车通过隧道时引起的压力瞬态。对比数值模拟和动模型试验得到的压力波动波形和最大峰峰值，选用了 SST k-ω 湍流模型和结构化网格数值模拟高速列车通过隧道的过程。数值模拟与动模试验的最大压力波振幅值相吻合。数值模拟的初始压缩波和膨胀波振幅最大的位置与动模试验的位置一致。测点的计算压力完全符合隧道中压缩波和膨胀波的传播规律。

关键词：高速列车；计算网格；湍流模型；隧道；压力波动